


Communication

# Non-Contact Oxygen Saturation Measurement Using YCgCr Color Space with an RGB Camera

Na Hye Kim <sup>1</sup>, Su-Gyeong Yu <sup>1</sup>, So-Eui Kim <sup>1</sup> and Eui Chul Lee <sup>2,\*</sup> 

<sup>1</sup> Department of AI & Informatics, Graduate School, Sangmyung University, Seoul 03016, Korea; 202032010@sangmyung.kr (N.H.K.); 202032015@sangmyung.kr (S.-G.Y.); 202032011@sangmyung.kr (S.-E.K.)

<sup>2</sup> Department of Human-Centered Artificial Intelligence, Sangmyung University, Seoul 03016, Korea

\* Correspondence: eclees@smu.ac.kr

**Abstract:** Oxygen saturation (SPO<sub>2</sub>) is an important indicator of health, and is usually measured by placing a pulse oximeter in contact with a finger or earlobe. However, this method has a problem in that the skin and the sensor must be in contact, and an additional light source is required. To solve these problems, we propose a non-contact oxygen saturation measurement technique that uses a single RGB camera in an ambient light environment. Utilizing the fact that oxygenated and deoxygenated hemoglobin have opposite absorption coefficients at green and red wavelengths, the color space of photoplethysmographic (PPG) signals recorded from the faces of study participants were converted to the YCgCr color space. Substituting the peaks and valleys extracted from the converted Cg and Cr PPG signals into the Beer–Lambert law yields the SPO<sub>2</sub> via a linear equation. When the non-contact SPO<sub>2</sub> measurement value was evaluated based on the reference SPO<sub>2</sub> measured with a pulse oximeter, the mean absolute error was 0.537, the root mean square error was 0.692, the Pearson correlation coefficient was 0.86, the cosine similarity was 0.99, and the intraclass correlation coefficient was 0.922. These results confirm the feasibility of non-contact SPO<sub>2</sub> measurements.



**Citation:** Kim, N.H.; Yu, S.-G.; Kim, S.-E.; Lee, E.C. Non-Contact Oxygen Saturation Measurement Using YCgCr Color Space with an RGB Camera. *Sensors* **2021**, *21*, 6120. <https://doi.org/10.3390/s21186120>

Academic Editor: Yu-Dong Zhang

Received: 9 August 2021

Accepted: 9 September 2021

Published: 12 September 2021

**Publisher's Note:** MDPI stays neutral with regard to jurisdictional claims in published maps and institutional affiliations.



**Copyright:** © 2021 by the authors. Licensee MDPI, Basel, Switzerland. This article is an open access article distributed under the terms and conditions of the Creative Commons Attribution (CC BY) license (<https://creativecommons.org/licenses/by/4.0/>).

**Keywords:** oxygen saturation; YCgCr color space; hemoglobin; Beer-Lambert law; photoplethysmographic signal

## 1. Introduction

Blood oxygen saturation (SPO<sub>2</sub>) refers to the concentration of oxygenated hemoglobin relative to the total amount of hemoglobin in the blood. A normal blood oxygen saturation level is 95–100% at sea level and falls below 90% due to hypoxemia or other reasons. Severe hypoxemia (SPO<sub>2</sub> < 80%) can have serious implications for the brain, heart, and lungs, and requires immediate attention [1]. In addition, COVID-19 patients who often show low SPO<sub>2</sub> (SPO<sub>2</sub> < 90%) are hospitalized, and SPO<sub>2</sub> has been used as an indicator in the diagnosis of COVID-19 [2]. SPO<sub>2</sub> is an important indicator of health and can be used in the early-stage detection of respiratory diseases. The current standard for SPO<sub>2</sub> measurement is pulse oximetry using the photoplethysmographic (PPG) method, which measures changes in blood volume through the amount of light transmitted or reflected after irradiating the skin with light. Using this measurement method and the fact that oxygenated hemoglobin and deoxygenated hemoglobin absorb red and infrared light differently, the sensor is contacted with the patient's body, typically the finger or ear lobe [3]. However, this method requires infrared and red-light illumination and contact with the sensor, with the latter potentially causing discomfort and skin irritation. Moreover, when sensors are attached to body parts, participants can consciously or unconsciously influence oxygen saturation values because they are aware that they are being monitored. Therefore, in this study, we propose a non-contact method for measuring SPO<sub>2</sub>.

Previous studies involving photoplethysmographic (PPG)-based SPO<sub>2</sub> measurements have proposed using light sources with specific wavelengths and multiple cameras. For

example, Kong et al. proposed an SPO<sub>2</sub> measurement method that uses light with wavelengths of 520 nm and 660 nm. To use two wavelengths of light, the signals were extracted by photographing faces through two cameras with narrow-pass filters. After determining the alternating current (AC)/direct current (DC) signal ratio at both wavelengths, the SPO<sub>2</sub> was measured through calibration [4]. Tamura also used the ratio method, but with 660 nm (red) and 940 nm (infrared) light sources [5]. However, in this paper, we propose a non-contact SPO<sub>2</sub> measurement technique that uses ambient light through a single RGB camera without requiring additional illumination.

In order to measure SPO<sub>2</sub> in a non-contact manner, it is necessary to measure a heart signal, that is, a PPG signal, in a non-contact manner. In general, the PPG signal is obtained by attaching a sensor to the skin and measuring the amount of transmitted light by emitting light. However, this method has the inconvenience of having to attach a sensor to the body. Therefore, studies on remote PPG (rPPG), a technology for measuring PPG signals in a non-contact manner using a camera, are being conducted. Verkruyse et al. proposed a method for measuring heart rate using ambient light and a digital camera and showed that the green channel contains the strongest plethysmography signal because hemoglobin absorbs green light the most, and green light can penetrate deep into the skin. In addition, it was shown that the red and blue channels also contain plethysmography information [6]. In the paper of Poh et al., it was explained that the RGB color sensor is mixed with the original signal with different weights for each color because the absorption rate of hemoglobin is different at each wavelength. Therefore, using Independent Component Analysis (ICA), the color channels were separated into independent components in the RGB image of the face, and the heart rate was extracted through this method [7]. Song et al. proposed an rPPG method showing excellent performance against noise by mapping between spatiotemporal heart rate (HR) feature images and corresponding HR values using CNN [8]. These existing rPPG technologies are focused on calculating heart rate rather than extracting rPPG raw signals, as it is difficult to measure SPO<sub>2</sub> using rPPG raw signals. Recently, Allado et al. proposed a method to obtain physiological variables such as heart rate, respiratory, and oxygen saturation by obtaining raw data through red, green, and blue color spectra measurement from face images [9]. Like this study, research on raw data analysis has been conducted recently, but detailed algorithms for extracting vital signs such as oxygen saturation using raw data and quality of raw signals are unknown.

Unlike previous studies, lab-made rPPG technology can extract rPPG raw signals in real time, so bio-markers such as HR and SPO<sub>2</sub> can be extracted from this signal. Since this technology extracts the rPPG signal from the color image, SPO<sub>2</sub> can be obtained using this RGB raw signal. Therefore, it is possible to implement a non-contact system capable of SPO<sub>2</sub> analysis in real time beyond the level of rPPG technology that simply extracts heart rate.

We can extract the raw PPG signal in a non-contact manner, which is essential for measuring oxygen saturation in a non-contact manner. In addition, this method does not cause inconvenience when measuring oxygen saturation in a contact manner. Therefore, this paper proposes a method for measuring oxygen saturation in a non-contact manner. The remainder of this paper proceeds as follows. Section 2 explains the SPO<sub>2</sub> measurement principle, PPG signal extraction, and the SPO<sub>2</sub> measurement method. In Section 3, the results are analyzed by comparing SPO<sub>2</sub> measurements acquired using the conventional sensor-based method with those acquired using our proposed method. Section 4 analyzes the results and describes the need for further research. Finally, Section 5 presents the research conclusion and future research.

## 2. Methods

### 2.1. Oxygen Saturation Measurement Principle

Camera-based SPO<sub>2</sub> measurements use PPG and the Beer–Lambert law. In PPG, blood flow is determined according to the amount of incident light that is reflected or transmitted [10]. Blood flow affects not only the reflectance but also the type and con-

centration of substances in the blood. As shown in Figure 1, in the case of green light, oxygenated hemoglobin absorbs green light more strongly than deoxygenated hemoglobin. On the other hand, in the case of red light, deoxygenated hemoglobin absorbs red light more strongly than oxygenated hemoglobin [11]. This wavelength-dependent behavior of hemoglobin absorption can be used to measure SPO<sub>2</sub>. In addition, PPG signals contain both an alternating current (AC), a pulsatile waveform caused by heartbeats, and a direct current (DC), a non-pulsatile waveform caused by veins, other tissues, artifacts, and the respiratory modulation [12]. Since SPO<sub>2</sub> is measured using pulse changes in the arteries, we use an AC component.

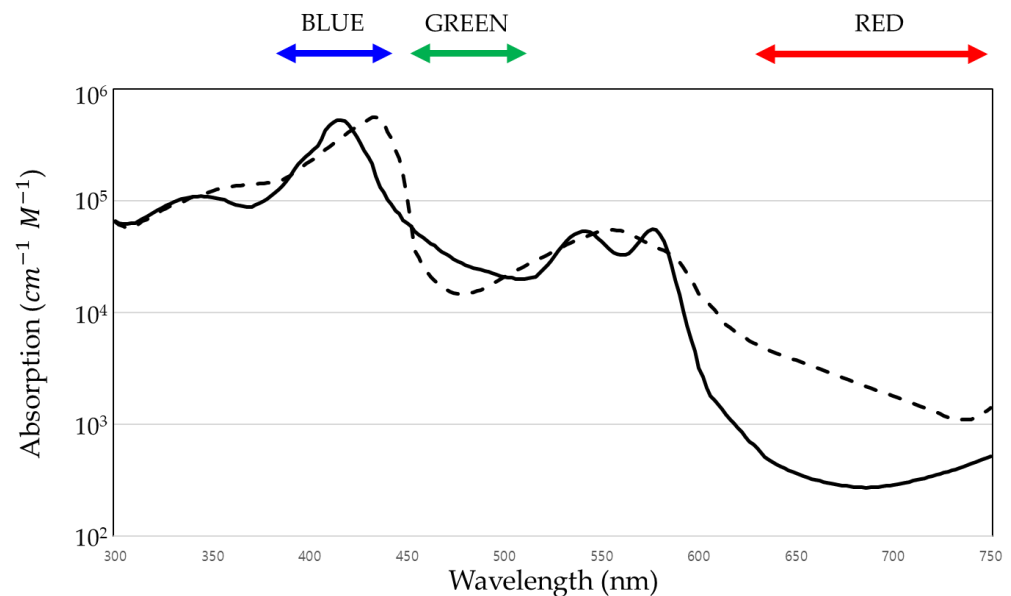


**Figure 1.** Wavelength-dependent absorption coefficients of oxygenated (solid line) and deoxygenated hemoglobin (dashed line).

The Beer–Lambert law states that the absorption of light is proportional to the concentration of the substance and the optical penetration depth [13]. It is expressed as:

$$I = I_0 e^{-\varepsilon(\lambda)Cl}, \quad (1)$$

where  $I$  is the reflected light intensity,  $I_0$  is the incident light intensity,  $\varepsilon(\lambda)$  is the absorption coefficient at wavelength  $\lambda$ ,  $C$  is the concentration, and  $l$  is the optical path length. Using Equation (1), the concentration of oxygenated hemoglobin and deoxygenated hemoglobin in the blood can be obtained through the intensity of reflected light. The SPO<sub>2</sub> is calculated by using this law and the AC component of the PPG.

## 2.2. Non-Contact SPO<sub>2</sub> Measurement Method

The proposed non-contact SPO<sub>2</sub> measurement process is shown in Figure 2. The PPG signal is extracted from the camera and the SPO<sub>2</sub> is calculated based on the extracted signal. To extract the PPG signal from the camera, face image data were captured for 5 min using an RGB camera [14]. At the same time, reference SPO<sub>2</sub> data were obtained by attaching a CMS-50E [15] pulse oximeter to the participant's finger. During the experiment, hypoxia was induced by instructing participants to hold their breath for 1 min, reducing SPO<sub>2</sub> by an average of 10%. A total of 10 healthy Koreans (5 males and 5 females) aged 23 to 31 years took part in the study. Before the experiment, subjects were instructed to minimize finger and facial movements and not to put on makeup to prevent noise. The experiment was conducted in an indoor environment with an average temperature of 20 to 24 °C, average humidity of 50% to 60%, and an average brightness of 500 lux. The research followed

the principle of the Declaration of Helsinki, and informed consent was obtained from the subjects after an explanation of nature.

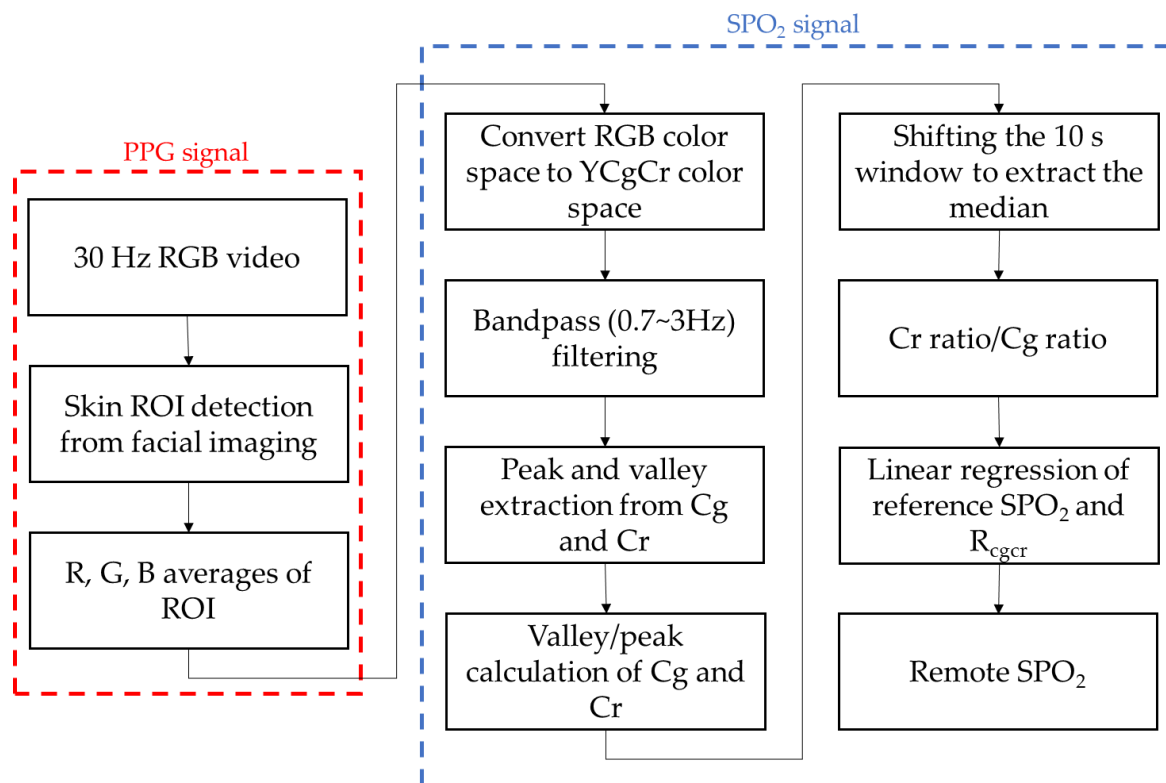


**Figure 2.** Non-contact oxygen saturation measurement process. R = red; B = blue; G = green; ROI = region of interest;  $R_{cgcr}$  = Cr ratio/Cg ratio.

The process of extracting the PPG signal is explained in Section 2.2.1, while the process of determining the  $SPO_2$  from the extracted signal is described in Section 2.2.2.

### 2.2.1. Remote PPG Signal

Non-contact  $SPO_2$  measurements necessitate non-contact PPG signal measurements. To obtain a non-contact PPG signal, we used lab-made remote-PPG (rPPG) technology developed in-house that can measure PPG signals in real time using a camera [16]. Specifically, our lab-made system measures the PPG signal according to blood flow-induced changes in skin color. This technique obtains PPG signals as follows. First, a face is detected in an RGB image frame at 30 frames per second and then tracked in a continuous image frame using a kernelized correlation filter (KCF) tracker [17]. To observe changes in skin color, a specific region of skin on the detected face is selected as the region of interest (ROI). In this case, if a face region excluding the background is simply selected, the intensity of the blood flow signal is minute, and the signal may be distorted due to noise caused by lighting changes and artifacts. Therefore, after converting the image frame from the RGB color space to the YCbCr color space, skin pixel clustering is performed in the Cb-Cr plane to utilize the skin pixel characteristics. The ROI of the selected face region means the entire skin area of the face except for eyebrows, eyes, and accessories such as glasses. This is because if the ROI is small, it will be greatly affected by noise, such as the natural tremor of a person, and if the ROI is the forehead, there is a risk that it will be covered with hair. Next, the PPG signal is extracted by calculating the average of each of R, G, and B in the selected ROI of each frame. The rPPG signal extraction process is summarized in Figure 3, and the real-time rPPG signal extraction can be viewed in the Supporting Information of the video by [18].

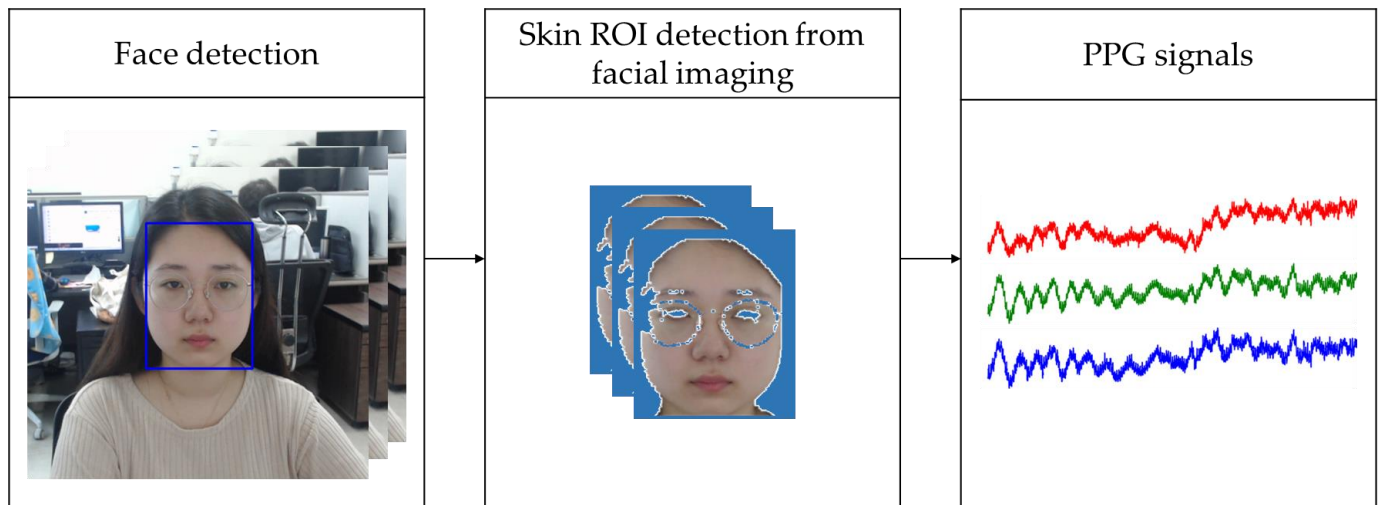


**Figure 3.** PPG signal acquisition process. The red line is the R raw signal, the green line is the G raw signal, and the blue line is B raw signal.

### 2.2.2. SPO<sub>2</sub> Signal

#### SPO<sub>2</sub> Measurement Using YCgCr Signal

The RGB color space is converted to the YCgCr color space by applying Equation (2) [19] to the PPG signal extracted in Section 2.2.1. Y is the luminance component, and Cg and Cr are the green-difference and red-difference chroma components, respectively. In Equation (2), R', G', and B' represent the values of R, G, and B, respectively, normalized to a value between 0 and 1 by dividing by the maximum pixel value of 255:

$$\begin{aligned} Y &= 16 + (65.481 \times R') + (128.533 \times G') + (24.966 \times B') \\ C_g &= 128 + (-81.085 \times R') + (112 \times G') + (-30.915 \times B') \\ C_r &= 128 + (112 \times R') + (-93.786 \times G') + (-18.214 \times B') \end{aligned} \quad (2)$$

SPO<sub>2</sub> is measured using two or more wavelengths of light and utilizing the different absorption characteristics of different types of hemoglobin. At green and red wavelengths, the absorption of oxygenated and deoxygenated hemoglobin exhibit opposite responses. Therefore, we chose to use these wavelengths for our study. The RGB color space was converted to the YCgCr color space to eliminate the effect of light brightness and use these green and red wavelengths. To extract the heartbeat-related signals covering the entire span of the expected physiological heart rate range from the converted Cg and Cr signals, bandpass filtering was applied to pass only frequencies ranging 0.7–3 Hz (corresponding to 42 to 180 beats/min). In this case, bandpass filtering was performed using a zero-phase five-order Butterworth filter [20]. Based on our use of brightness-independent Cg and Cr signals, the Beer–Lambert law in Equation (1) was modified to Equation (3) to calculate the SPO<sub>2</sub>:

$$I = e^{-\epsilon(\lambda)Cl} \quad (3)$$

In the filtered AC signals of Cg and Cr, the maximum (minimum) amplitudes are denoted as I<sub>cg,p</sub> and I<sub>cr,p</sub> (I<sub>cg,v</sub> and I<sub>cr,v</sub>), respectively. In accordance with Equation (3), this can be expressed as:

$$I_{cg,p} = e^{-[\epsilon_{Hb}(\lambda_{cg})C_{Hb} + \epsilon_{HbO_2}(\lambda_{cg})C_{HbO_2}]l}, \quad (4)$$

$$I_{cg,v} = e^{-[\epsilon_{Hb}(\lambda_{cg})C_{Hb} + \epsilon_{HbO_2}(\lambda_{cg})C_{HbO_2}](1+\Delta l)}, \quad (5)$$

$$I_{cr,p} = e^{-[\epsilon_{Hb}(\lambda_{cr})C_{Hb} + \epsilon_{HbO_2}(\lambda_{cr})C_{HbO_2}]l}, \quad (6)$$

$$I_{cr,v} = e^{-[\epsilon_{Hb}(\lambda_{cr})C_{Hb} + \epsilon_{HbO_2}(\lambda_{cr})C_{HbO_2}](1+\Delta l)}, \quad (7)$$

where  $\varepsilon_{\text{Hb}}(\lambda_{\text{cg}})C_{\text{Hb}}$  and  $\varepsilon_{\text{Hb}}(\lambda_{\text{cr}})C_{\text{Hb}}$  are the products of the absorption coefficient and concentration of deoxygenated hemoglobin at the Cg and Cr wavelengths.  $\varepsilon_{\text{HbO}_2}(\lambda_{\text{cg}})C_{\text{HbO}_2}$  and  $\varepsilon_{\text{HbO}_2}(\lambda_{\text{cr}})C_{\text{HbO}_2}$  are the products of the absorption coefficient and concentration of oxygenated hemoglobin at the Cg and Cr wavelengths.  $l$  and  $\Delta l$  are the light penetration depth in the arteries, which indicates the volume of blood.  $l$  means the thickness of the thinnest arterial blood vessel, that is, when the blood flow is the minimum.  $\Delta l$  is the change in blood flow due to heartbeat. Because the volume of blood and the reflected light intensity are inversely proportional, the reflected light intensity corresponding to the smallest blood volume is used to calculate the peak point in Equations (4) and (6). In addition, when calculating the valley point in Equations (5) and (7),  $l + \Delta l$ , which represents the case of increased blood volume, is used. The  $\text{SPO}_2$  can be measured in the part that fluctuates with the heartbeat. Therefore, as in Equations (8) and (9), only the effect of hemoglobin is left in the part that is changed by the heartbeat through the logarithm of the ratio of peak to valley.

$$\ln\left(\frac{I_{\text{cg},v}}{I_{\text{cg},p}}\right) = -[\varepsilon_{\text{Hb}}(\lambda_{\text{cg}})C_{\text{Hb}} + \varepsilon_{\text{HbO}_2}(\lambda_{\text{cg}})C_{\text{HbO}_2}]\Delta l, \quad (8)$$

$$\ln\left(\frac{I_{\text{cr},v}}{I_{\text{cr},p}}\right) = -[\varepsilon_{\text{Hb}}(\lambda_{\text{cr}})C_{\text{Hb}} + \varepsilon_{\text{HbO}_2}(\lambda_{\text{cr}})C_{\text{HbO}_2}]\Delta l. \quad (9)$$

Then, to reduce noise caused by other factors excepting for oxygen saturation, the logarithmic function was applied in such a way that the median value was extracted when the 10-s window was moved at one sample interval. However, the effect of fluctuating blood volume remains. As shown in Figure 4d, it can be confirmed that the Cg and Cr ratios reflect changes in  $\text{SPO}_2$  but contain a large number of high-frequency noise components due to heartbeat. To eliminate this effect, the ratio of two different wavelengths is obtained:

$$R_{\text{cgcr}} = \frac{\ln\left(\frac{I_{\text{cr},v}}{I_{\text{cr},p}}\right)}{\ln\left(\frac{I_{\text{cg},v}}{I_{\text{cg},p}}\right)} = \frac{\varepsilon_{\text{Hb}}(\lambda_{\text{cr}})C_{\text{Hb}} + \varepsilon_{\text{HbO}_2}(\lambda_{\text{cr}})C_{\text{HbO}_2}}{\varepsilon_{\text{Hb}}(\lambda_{\text{cg}})C_{\text{Hb}} + \varepsilon_{\text{HbO}_2}(\lambda_{\text{cg}})C_{\text{HbO}_2}}. \quad (10)$$

As a result, only the effect of hemoglobin according to the wavelength remains, and  $\text{SPO}_2$  can be obtained. Note that  $R_{\text{cgcr}}$  was calibrated using the linear regression between the obtained  $R_{\text{cgcr}}$  value and the reference  $\text{SPO}_2$  level.

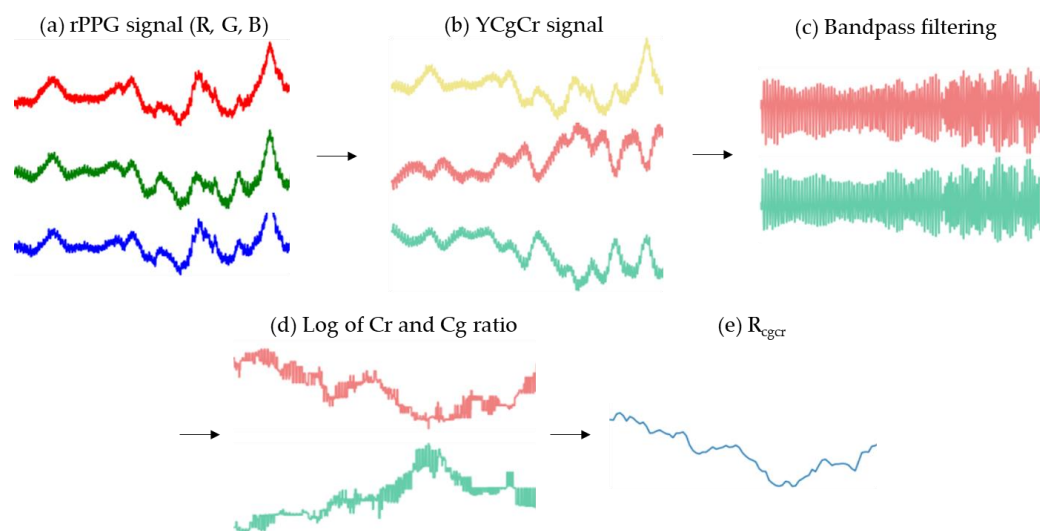


**Figure 4.** Process of extracting  $R_{\text{cgcr}}$  value from rPPG signal (a) R, G, B signals extracted from face ROI. The red line is the R raw signal, the green line is the G raw signal, and the blue line is B raw signal. (b) R, G, B signals are converted into YCgCr color space. The yellow line is the Y signal, the pink line is the Cr signal, and the light blue line is the Cg signal. (c) Result of bandpass filtering on

Cg and Cr signals. The pink line is the filtered Cr signal, the light blue line is the filtered Cg signal. (d) The result of Equations (8) and (9). That is, the log value of the peak/valley extracted from the Cg and Cr signals to which bandpass filtering is applied, respectively. The pink line is the calculated Cr signal, the light blue line is the calculated Cg signal. (e) The result of Equation (10), that is, Cr ratio/Cg ratio.

### SPO<sub>2</sub> Measurement Using YCbCr Signal

As shown in Figure 1, there is a part where the absorption coefficients of non-oxygenated hemoglobin and oxygenated hemoglobin are opposite to each other at blue and red wavelengths. Therefore, oxygen saturation can be measured using blue and red wavelengths. To apply this fact, after converting the RGB color space of the rPPG signal to YCbCr, the blue-difference chroma component Cb and the red-difference chroma component Cr signal are extracted. After calculating the extracted Cb and Cr signals as described above to obtain the  $R_{cbcr}$  value and performing linear regression with the reference SPO<sub>2</sub>, SPO<sub>2</sub> can be obtained by calibrating these values.

## 3. Results

### 3.1. Correlation between $R_{cgcr}$ Value Obtained Using YCgCr Signal and Reference SPO<sub>2</sub>

The  $R_{cgcr}$  values were obtained from the face image recorded using the method described in Section 2.2. The  $R_{cgcr}$  values were calibrated to obtain the remote SPO<sub>2</sub> (rSPO<sub>2</sub>). However, prior to this calibration, the Pearson correlation coefficient was calculated to ascertain whether a linear relationship existed between the  $R_{cgcr}$  value and the reference SPO<sub>2</sub>. As shown in Figure 5, a Pearson's correlation coefficient of 0.86 was determined, confirming the linear correlation between the  $R_{cgcr}$  value and the reference SPO<sub>2</sub>. The reason blue dots appear as horizontal lines in Figure 5 is that the reference SPO<sub>2</sub> value is measured as an integer, but the  $R_{cgcr}$  value is measured as a continuous real number.

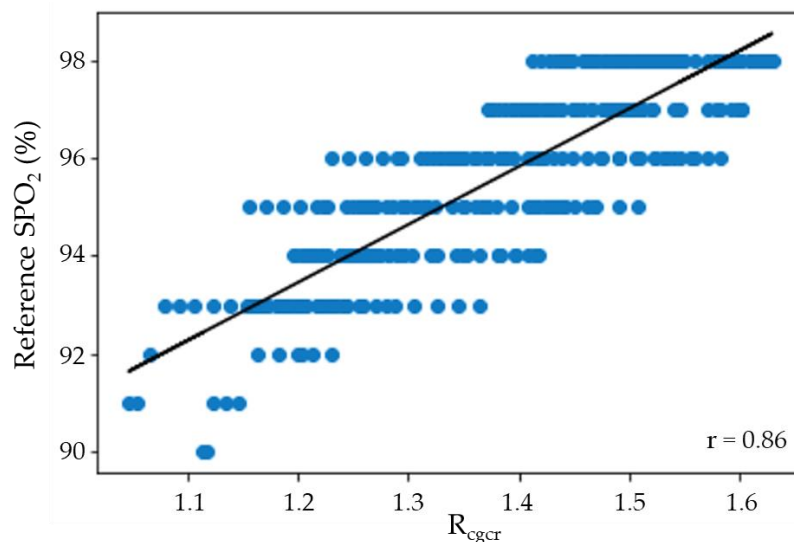


**Figure 5.** Scatter plot showing the relationship between  $R_{cgcr}$  and the reference SPO<sub>2</sub>.

After this linear relationship was confirmed, the  $R_{cgcr}$  values were derived from Equation (11) through linear regression with the reference SPO<sub>2</sub> and corrected for rSPO<sub>2</sub><sup>cgcr</sup>.

$$rSPO_2^{cgcr} = 11.8805 \times R_{cgcr} + 79.1914. \quad (11)$$

### 3.2. Correlation between R<sub>cbcr</sub> Value Obtained Using YCbCr Signal and Reference SPO<sub>2</sub>

The R<sub>cbcr</sub> value was obtained by converting the RGB color space of the rPPG signal to YCbCr. Now, by calibrating this R<sub>cbcr</sub> value, rSPO<sub>2</sub><sup>cbcr</sup> can be obtained. Before calibration, Pearson's correlation coefficient was obtained to check whether there is any relationship between the R<sub>cbcr</sub> value and the reference SPO<sub>2</sub>. As a result, 0.27 was obtained, and the following Equation (12) was derived through linear regression with reference SPO<sub>2</sub>.

$$rSPO_2^{cbcr} = 7.40325 \times R_{cgr} + 87.9765. \quad (12)$$

### 3.3. Comparison of rSPO<sub>2</sub> and Reference SPO<sub>2</sub>

Figure 6 compares rSPO<sub>2</sub> measured using CgCr and rSPO<sub>2</sub> measured using CbCr with reference SPO<sub>2</sub>. It can be confirmed that rSPO<sub>2</sub> measured using Cg and Cr was better estimated when compared with reference SPO<sub>2</sub> than rSPO<sub>2</sub> measured using Cb and Cr. However, to confirm this quantitatively, mean absolute error (MAE), root mean squared error (RMSE), cosine similarity, and intraclass correlation coefficient (ICC) [21] were used. These results can be seen in Table 1. MAE and RMSE for calculating the distance between reference SPO<sub>2</sub> and rSPO<sub>2</sub> are 0.537 and 0.692 for rSPO<sub>2</sub><sup>cgr</sup>, respectively, which are smaller than 1.547 and 1.754 for rSPO<sub>2</sub><sup>cbcr</sup>. This indicates that the absolute difference between rSPO<sub>2</sub><sup>cgr</sup> and reference SPO<sub>2</sub> is small, indicating that rSPO<sub>2</sub><sup>cgr</sup> was predicted better than rSPO<sub>2</sub><sup>cbcr</sup>. In the ICC 95% confidence interval, rSPO<sub>2</sub><sup>cgr</sup> was 0.922 and rSPO<sub>2</sub><sup>cbcr</sup> was 0.243. This means that in the case of rSPO<sub>2</sub><sup>cgr</sup>, it is 92.2% identical to the reference SPO<sub>2</sub>, and in the case of rSPO<sub>2</sub><sup>cbcr</sup>, it is 24.3% identical. At this time, in the case of rSPO<sub>2</sub><sup>cgr</sup>, it is statistically significant because the significance probability is less than 0.001. The cosine similarity shows how similar the directions of the two vectors are, and 0.999 was obtained for both rSPO<sub>2</sub><sup>cgr</sup> and rSPO<sub>2</sub><sup>cbcr</sup>. It can be seen that when the reference SPO<sub>2</sub> decreases, rSPO<sub>2</sub> also decreases, and vice versa. However, as shown in Figure 6, in the case of rSPO<sub>2</sub><sup>cbcr</sup>, the trend may be similar, but the error is large, so MAE and RMSE should be considered together to determine whether rSPO<sub>2</sub> is well predicted. Therefore, as shown in the statistical results, it can be seen that rSPO<sub>2</sub><sup>cgr</sup> predicted SPO<sub>2</sub> well.

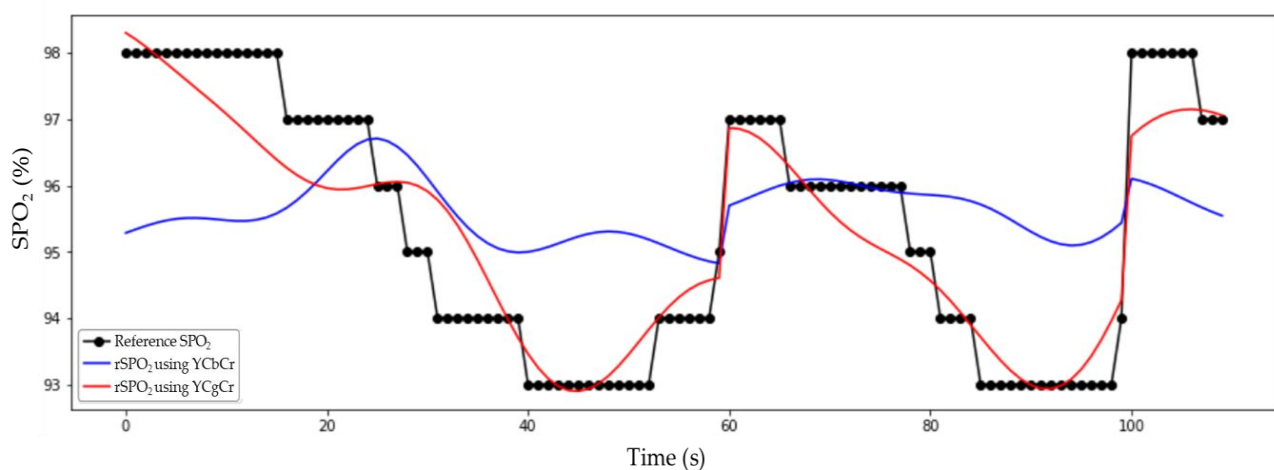


**Figure 6.** Comparison of rSPO<sub>2</sub> obtained by non-contact and reference SPO<sub>2</sub> obtained by contact sensor. The black line is the reference SPO<sub>2</sub>, the red line is the rSPO<sub>2</sub><sup>cgr</sup>, and the blue line is the rSPO<sub>2</sub><sup>cbcr</sup>.

**Table 1.** Statistical results of rSPO<sub>2</sub><sup>cgr</sup> and rSPO<sub>2</sub><sup>cbcr</sup>. MAE = mean absolute error; RMSE = root mean squared error.

	MAE	RMSE	Cosine Similarity	Intraclass Correlation Coefficient		
				Intraclass Correlation	95% Confidence Interval	Sig
rSPO <sub>2</sub> <sup>cgr</sup>	0.537 (±0.436)	0.692	0.999	0.922	0.905–0.936	0.000
rSPO <sub>2</sub> <sup>cbcr</sup>	1.547 (±0.827)	1.754	0.999	0.243	0.075–0.381	0.003



#### 4. Discussion

In this paper, we proposed a method to measure oxygen saturation in a non-contact manner by extracting a remote PPG signal. There are two methods for measuring SPO<sub>2</sub> in a non-contact manner, one using the Cg and Cr signal and the other using the Cb and Cr signal. Consequently, the use of Cg and Cr signals is recommended. This study measures SPO<sub>2</sub> using an RGB camera in ambient light, which has a broadband spectral response rather than a narrowband spectral response. This is because the absorption coefficients of the two hemoglobin are opposite at the blue and red wavelengths only in the narrowband of blue. Therefore, the method using the Cb and Cr signal does not utilize the characteristic that the absorption coefficients of non-oxygenated hemoglobin and oxygenated hemoglobin are opposite at different wavelengths, so the results are not good.

There are several factors that can be improved in the future. We calculated the oxygen saturation from the raw R, G, and B signals in the rPPG signal. This raw signal contains motion artifacts and noise, but no other processing than frequency filtering is performed, so noise such as motion may affect the quality of the signal. Therefore, if motion information is obtained through the camera and additional pre-processing is performed, a motion robust signal can be obtained. Furthermore, this study involved SPO<sub>2</sub> levels of 85–100% because the SPO<sub>2</sub> value was lowered deliberately by instructing participants to hold their breath. In the future, it is necessary to further lower the SPO<sub>2</sub> level and develop a proposed method to broaden the measurement range of the non-contact method.

#### 5. Conclusions

This paper describes a technique for non-contact SPO<sub>2</sub> measurements using a single RGB camera under ambient light conditions. In this study, we utilized the opposite absorption characteristics of hemoglobin at the green and red wavelengths. Consequently, the Cg and Cr signals were extracted by converting the RGB color space of the PPG signal extracted from facial images to the YCgCr color space. After obtaining AC signals from each of the extracted Cg and Cr signals, find the peak and valley points and take the logarithm of the peak/valley ratio. These values move the 10-s window at 1-sample intervals and extract the median value, and calculate the R<sub>cgcr</sub> value through the Cr/Cg ratio. The rSPO<sub>2</sub> was obtained by applying the linear regression-extracted equation to the resultant R<sub>cgcr</sub> value. Comparing the measured rSPO<sub>2</sub><sup>CGCr</sup> with the reference SPO<sub>2</sub> data, the MAE was 0.537, the RMSE was 0.692, the Pearson's correlation coefficient was 0.86, the cosine similarity was 0.99, and the ICC was 0.922. These results indicate that the SPO<sub>2</sub> measured by the proposed non-contact method is consistent with SPO<sub>2</sub> measurements acquired via conventional methods involving the attachment of a sensor, thus confirming the feasibility of accurate non-contact SPO<sub>2</sub> measurements. In future works, we plan to conduct a wide range of oxygen saturation measurement studies using critically ill patient data for clinical research. In other words, by extending the value range of SPO<sub>2</sub> ground-truth, the correlation with rPPG will be more clearly identified. In addition, further studies will be conducted to improve the speed of extraction of rPPG signals to obtain oxygen saturation.

**Author Contributions:** Conceptualization, E.C.L.; methodology, E.C.L. and N.H.K.; software, N.H.K.; validation, N.H.K. and S.-E.K.; investigation, N.H.K. and S.-G.Y.; data curation, N.H.K. and S.-E.K.; writing—original draft preparation, N.H.K.; writing—review and editing, E.C.L.; visualization, N.H.K. and S.-G.Y.; supervision, E.C.L.; project administration, E.C.L.; funding acquisition, E.C.L. All authors have read and agreed to the published version of the manuscript.

**Funding:** This work was supported by the NRF (National Research Foundation) of Korea funded by the Korea government (Ministry of Science and ICT) (NRF-2019R1A2C4070681). This work was also supported by the Industrial Strategic Technology Development Program (10073159, Developing mirroring expression based interactive robot technique by non-contact sensing and recognizing human intrinsic parameter for emotion healing through heart-body feedback) funded by the Ministry of Trade, Industry, and Energy (MI, Korea).

**Institutional Review Board Statement:** Based on the 13-1-3 of the Enforcement Regulations of the Act on Bioethics and Safety of the Republic of Korea, ethical review and approval were waived (IRB-SMU-S-2021-1-005) for this study by the Sangmyung University Institutional Review Board, because this study uses only simple contact measuring equipment or observation equipment that does not follow physical changes.

**Informed Consent Statement:** Informed consent was obtained from all subjects involved in the study.

**Data Availability Statement:** The obtained data cannot be shared because it was agreed that they could be used only for this study.

**Conflicts of Interest:** The authors declare no conflict of interest.

## References

1. West, J.B. *Pulmonary Pathophysiology: The Essentials*; Lippincott Williams & Wilkins: Philadelphia, PA, USA, 2011.
2. Caputo, N.D.; Strayer, R.J.; Levitan, R. Early Self-Prone in Awake, Non-Intubated Patients in the Emergency Department: A Single ED's Experience During the COVID-19 Pandemic. *Acad. Emerg. Med.* **2020**, *27*, 375–378. [[CrossRef](#)] [[PubMed](#)]
3. Severinghaus, J.W. Takuo Aoyagi: Discovery of Pulse Oximetry. *Anesth. Analg.* **2007**, *105*, S1–S4. [[CrossRef](#)] [[PubMed](#)]
4. Kong, L.; Zhao, Y.; Dong, L.; Jian, Y.; Jin, X.; Li, B.; Feng, Y.; Liu, M.; Liu, X.; Wu, H. Non-Contact Detection of Oxygen Saturation Based on Visible Light Imaging Device Using Ambient Light. *Opt. Express* **2013**, *21*, 17464–17471. [[CrossRef](#)] [[PubMed](#)]
5. Tamura, T. Current Progress of Photoplethysmography and SPO2 for Health Monitoring. *Biomed. Eng. Lett.* **2019**, *9*, 21–36. [[CrossRef](#)] [[PubMed](#)]
6. Verkruysse, W.; Svaasand, L.O.; Nelson, J.S. Remote plethysmographic imaging using ambient light. *Opt. Express* **2008**, *16*, 21434–21445. [[CrossRef](#)] [[PubMed](#)]
7. Poh, M.Z.; McDuff, D.J.; Picard, R.W. Non-contact, automated cardiac pulse measurements using video imaging and blind source separation. *Opt. Express* **2010**, *18*, 10762–10774. [[CrossRef](#)] [[PubMed](#)]
8. Song, R.; Zhang, S.; Li, C.; Zhang, Y.; Cheng, J.; Chen, X. Heart rate estimation from facial videos using a spatiotemporal representation with convolutional neural networks. *IEEE Trans. Instrum. Meas.* **2020**, *69*, 7411–7421. [[CrossRef](#)]
9. Allado, E.; Poussel, M.; Moussu, A.; Saunier, V.; Bernard, Y.; Albuisson, E.; Chenuel, B. Innovative measurement of routine physiological variables (heart rate, respiratory rate and oxygen saturation) using a remote photoplethysmography imaging system: A prospective comparative trial protocol. *BMJ Open* **2021**, *11*, e047896. [[CrossRef](#)] [[PubMed](#)]
10. Allen, J. Photoplethysmography and Its Application in Clinical Physiological Measurement. *Physiol. Meas.* **2007**, *28*, R1–R39. [[CrossRef](#)] [[PubMed](#)]
11. Tabulated Molar Extinction Coefficient for Hemoglobin in Water. Available online: <https://omlc.org/spectra/hemoglobin/summary.html> (accessed on 10 August 2021).
12. Chan, E.D.; Chan, M.M.; Chan, M.M. Pulse Oximetry: Understanding Its Basic Principles Facilitates Appreciation of Its Limitations. *Respir. Med.* **2013**, *107*, 789–799. [[CrossRef](#)] [[PubMed](#)]
13. Swinehart, D.F. The Beer-Lambert Law. *J. Chem. Educ.* **1962**, *39*, 333. [[CrossRef](#)]
14. CMS50E Fingertip Pulse Oximeter. Available online: <https://www.cpap-supply.com/CMS50E-Pulse-Oximeter-p/cms50e.htm> (accessed on 10 August 2021).
15. Logitech. Available online: <https://www.logitech.com/ko-kr/products/webcams/c920-pro-hd-webcam.960-001062.html> (accessed on 10 August 2021).
16. Suh, K.H.; Lee, E.C. Contactless Physiological Signals Extraction Based on Skin Color Magnification. *J. Electron. Imaging* **2017**, *26*, 063003. [[CrossRef](#)]
17. Henriques, J.F.; Caseiro, R.; Martins, P.; Batista, J. High-speed tracking with kernelized correlation filters. *IEEE Trans. Pattern Anal. Mach. Intell.* **2014**, *37*, 583–596. [[CrossRef](#)] [[PubMed](#)]
18. Suh, G.H. oryong79, 18 May 2020. Real-Time rPPG with Facial Movements [Video File]. Available online: <https://www.youtube.com/watch?v=DWW8oS1YRLU> (accessed on 10 August 2021).
19. De Dios, J.J.; Garcia, N. Face Detection Based on a New Color Space YCgCr. In Proceedings of the International Conference on Image Processing (Cat No. 03CH37429), Barcelona, Spain, 14–17 September 2003; Volume 3.
20. Ali, A.S.; Radwan, A.G.; Soliman, A.M. Fractional order Butterworth filter: Active and passive realizations. *IEEE J. Emerg. Sel. Top. Circuits Syst.* **2013**, *3*, 346–354. [[CrossRef](#)]
21. Koo, T.K.; Li, M.Y. A Guideline of Selecting and Reporting Intraclass Correlation Coefficients for Reliability Research. *J. Chiropr. Med.* **2016**, *15*, 155–163. [[CrossRef](#)] [[PubMed](#)]